the plant journal

SEB SOCIETY FOR EXPERIMENTAL BIOLOGY

The Plant Journal (2023) **114,** 934–950 doi: 10.1111/tpj.16186

Begomoviral βC1 orchestrates organellar genomic instability to augment viral infection

Ashwin Nair[1,2], Chitthavalli Y. Harshith[1], Anushree Narjala[1,2] and Padubidri V. Shivaprasad[1,*]

[1]*National Centre for Biological Sciences, Tata Institute of Fundamental Research, GKVK Campus, Bellary Road, Bangalore 560065, India, and*

[2]*SASTRA University, Thirumalaisamudram, Thanjavur 613401, India*

Received 17 November 2022; revised 4 March 2023; accepted 10 March 2023; published online 14 March 2023.
*For correspondence (e-mail shivaprasad@ncbs.res.in).

SUMMARY

Chloroplast is the site for transforming light energy to chemical energy. It also acts as a production unit for a variety of defense-related molecules. These defense moieties are necessary to mount a successful counter defense against pathogens, including viruses. Previous studies indicated disruption of chloroplast homeostasis as a basic strategy of *Begomovirus* for its successful infection leading to the production of vein-clearing, mosaic, and chlorotic symptoms in infected plants. Although begomoviral pathogenicity determinant protein Beta C1 (βC1) was implicated for pathogenicity, the underlying mechanism was unclear. Here we show that, begomoviral βC1 directly interferes with the host plastid homeostasis. βC1 induced DPD1, an organelle-specific nuclease, implicated in nutrient salvage and senescence, as well as modulated the function of a major plastid genome maintainer protein RecA1, to subvert plastid genome. We show that βC1 was able to physically interact with bacterial RecA and its plant homolog RecA1, resulting in its altered activity. We observed that knocking-down *DPD1* during virus infection significantly reduced virus-induced necrosis. These results indicate the presence of a strategy in which a viral protein alters host defense by targeting modulators of chloroplast DNA. We predict that the mechanism identified here might have similarities in other plant–pathogen interactions.

Keywords: ***Begomovirus*, βC1, DNA-damage and repair, RecA, DPD1, chloroplast.**

INTRODUCTION

Chloroplast is an emerging hub for defense signaling during plant–pathogen interactions (de Torres Zabala et al., 2015; Nomura et al., 2012; Padmanabhan & Dinesh-Kumar, 2010; Serrano et al., 2016). In addition to being at the center for photosynthesis and various metabolic processes, chloroplast also synthesizes various immune modulators such as salicylic acid (SA), jasmonic acid, ethylene, abscisic acid, various secondary metabolites, aromatic amino acids, and other signaling molecules such as H_2O_2, reactive oxygen species (ROS, and singlet oxygen species $^1O_2$) (Chan et al., 2010; León & Sánchez-Serrano, 1999; Nambara & Marion-Poll, 2005; Wildermuth et al., 2001). The production of these immune modulators is tightly regulated to avoid dysfunctional expression leading to negative growth effects (Chandran et al., 2014).

Chloroplast consumes significant cellular resources. To accommodate the translational load, plastid genomes exist in multiple copies, and despite being relatively smaller, they account for the substantial DNA content of a plant cell (>20% in mature leaf) (Rauwolf et al., 2010; Sakamoto & Takami, 2018). Multiple copies of the plastid genome are essential for maintaining homeostasis during various metabolic processes (Bendich, 1987; Udy et al., 2012). The chloroplast genome is maintained by poorly studied organelle-specific DNA DAMAGE AND REPAIR (DDR) machinery, mostly encoded in the nucleus. A nucleoid proteome study identified a complex of 33 proteins involved in the homeostasis of chloroplast DNA (cpDNA) nucleoid (Majeran et al., 2012). The complex was enriched in replication (polymerase Ia, DNA gyrase A and B, etc.) and repair machinery (MutS, UV-REPAIR) proteins (UvrB/C), photolyases, and RecA orthologs. Most of the repair proteins involved in maintaining cpDNA was also known to be important for DNA-damage repair of nuclear genome. Orthologs of RecA protein such as RAD51 and RAD50 family members are crucial for nuclear double-stranded DNA break repair. Interestingly, proteins such as RecA1, RecA2, DRT100, and DRT102 are also orthologs of bacterial RecA, and are members of the DDR family that plays an essential

role in maintaining cpDNA. The DDR pathway proteins are essential for repair and maintenance of nuclear as well as plastid DNA (Kunkel, 2004; Majeran et al., 2012; Odahara et al., 2017; Rowan et al., 2010).

Begomovirus genera have a bipartite or monopartite genomic organization with two or more circular single-stranded (ss)DNA molecules. These molecules may be of equal size (DNA-A and DNA-B, bipartite) or a single DNA-A alone or with one or more satellite DNA molecules (monopartite). *Synedrella yellow vein clearing virus* (SyYVCV) is a vein clearing monopartite *Begomovirus* with a DNA-A along with a single satellite beta-satellite (DNA-β) (Das et al., 2018). The DNA-β cannot replicate independent of DNA-A. *Begomovirus* has been reported to accumulate in the host cell nucleus and depend on the host enzymes for replication (Schmid et al., 2014). Begomoviral particles are directly injected into the phloem by insect vectors surpassing the primary layer of defense in plants (Hanley-Bowdoin et al., 2013; Rizvi et al., 2015). However, recent studies indicated the activation of innate immunity upon geminiviral infection. The wounding response triggered by insect vector feeding can prime pattern triggered immunity and RNA-interference (Wang et al., 2021). In line with the role of chloroplast in antiviral defense, various viral effectors disrupt the key process of chloroplast metabolism to sabotage pattern triggered immunity activation (Bhattacharyya et al., 2015; Fondong et al., 2007; Gnanasekaran et al., 2019; Medina-Puche et al., 2020; Nair et al., 2020).

Begomoviruses employ robust mechanism for replication, involving both rolling-circle replication and recombination-dependent replication strategies. Rolling-circle replication is a robust process but also leads to the production of heterogeneous ssDNA of varying lengths due to polymerase runoff or improper termination (Heyraud et al., 1993; Heyraud-Nitschke et al., 1995; Stanley, 1995). Evidences such as the interaction of geminiviral Rep protein with host Rad54 (Kaliappan et al., 2012), and the role of host Rad51D (Richter et al., 2016) in maintaining the genomic integrity of the viral replicative forms (RFs) suggests the involvement of host DDR machinery during begomoviral replication (Ascencio-Ibáñez et al., 2008; Jeske et al., 2001; Preiss & Jeske, 2003). However, a clear understanding of these processes is lacking.

The transgenic expression of chloroplast-localized βC1 is toxic to plants (Cui et al., 2004; Yang et al., 2008). We and others had previously reported a multitude of growth defects observed in transgenic plants upon ectopic expression of βC1 (Bhattacharyya et al., 2015; Briddon et al., 2003; Cheng et al., 2011; Nair et al., 2020). Here we show that SyYVCV βC1 modulate specific set of DDR genes in host plants. It also induced selective degradation of cpDNA without significantly affecting nuclear DNA during viral infection. βC1 achieved this by inducing expression of chloroplast-specific nuclease named DPD1. βC1 was also able to interact and modulate the function of RecA1, a chloroplastic DDR protein in plants and its ortholog RecA in bacteria. Interaction of βC1 with RecA1 was paramount for successful viral pathogenesis in increasing the viral titer and for the formation of symptoms. We further show that βC1 can induce genotoxic stress. Our results indicate that interaction of βC1 protein with a DDR protein RecA1 and its influence on genotoxicity is another novel aspect of the much-appreciated arms race between viruses and their host plants.

RESULTS

βC1 alters the expression of key regulatory genes in βC1-expressing plants

The βC1-expressing transgenic tobacco plants were sterile, stunted, chlorotic, and presented an early flowering phenotype with exerted stigma (Figure 1a,b) (see also Nair et al., 2020). As observed previously, the toxicity of the βC1

Figure 1. βC1 Selectively induces degradation of chloroplastic DNA.
(a) Phenotype of transgenic *Nicotiana tabacum* lines overexpressing βC1. Pictures taken at 50 days post-transplantation. $N = 3$ for each transgenic line. Green fluorescent protein (GFP) VC is a GFP expressing vector control plant. Number in labels represents transgenic line number.
(b) Pictures of flower and seedpod.
(c) *Nicotiana tabacum* leaves showing necrosis when infected with DNA-A, DNA-A + β, and DNA-A + β-mβC1 (left). Heat map representing the extent of necrosis (right).
(d) Semi-quantitative DNA polymerase chain reaction showing abundance and integrity of chloroplastic (psbM+rpoB) or nuclear (actin) genome upon infection with β or β-mβC1 performed as observed in (c). R represents biological replicate number. β-mβC1 is DNA-β with inactive βC1, mutated in SIM motifs.
(e) Southern blot showing the intactness of chloroplastic genome in βC1 OE plants. A 3-kb (psbM+rpoB) chloroplastic region was used as a probe. Genomic DNA panel represents a duplicate gel with same amount of DNA used in Southern blot for normalization. βC1-DM is C-terminal GFP tagged defective βC1. WT, wild type.
(f) DNA quantitative polymerase chain reaction representing the abundance of chloroplastic (ycf3) or nuclear (PP2A) genes upon infection with β or β-mβC1. Nuclear actin was used for normalization.
(g) Same as (f) except 9 days post-inoculation (DPI) sample, with other plastid genes.
(h) Expression of DPD1 nuclease in virus infected samples with βC1 and mβC1.
(i) Phenotype of the systemic leaf expressing NtDPD1 (PVX-NtDPD1). 25 DPI. $N = 4$, image linked with Figure S2. Vector is empty PVX.
(j) (First panel, left to right) Schematics of infection on *N. tabacum* leaves. Necrotic phenotype of *N.* tabacum leaves infected with DNA-A, DNA-A + β, or β-mβC1 co-infiltrated with "X." "X" represents (second panel) PVX vector, (third panel) PVX-DPD1 or (fourth panel) PVX-anti-DPD1. White arrow highlights new necrotic spots. Pictures taken at 9 DPI. Biologically replicated, linked with Figure S2. Scale bar 2 cm. Additional information: N-terminal GFP tagged βC1 was used for generating transgenic βC1 lines. Size bar in (a) and (b) corresponds to 5.8, and 1 cm. Size bar in (c,i,j) is 1.2 cm. Tukey's multiple comparison test, $***P \leq 0.001$ and $**P \leq 0.01$. $n = 4$.

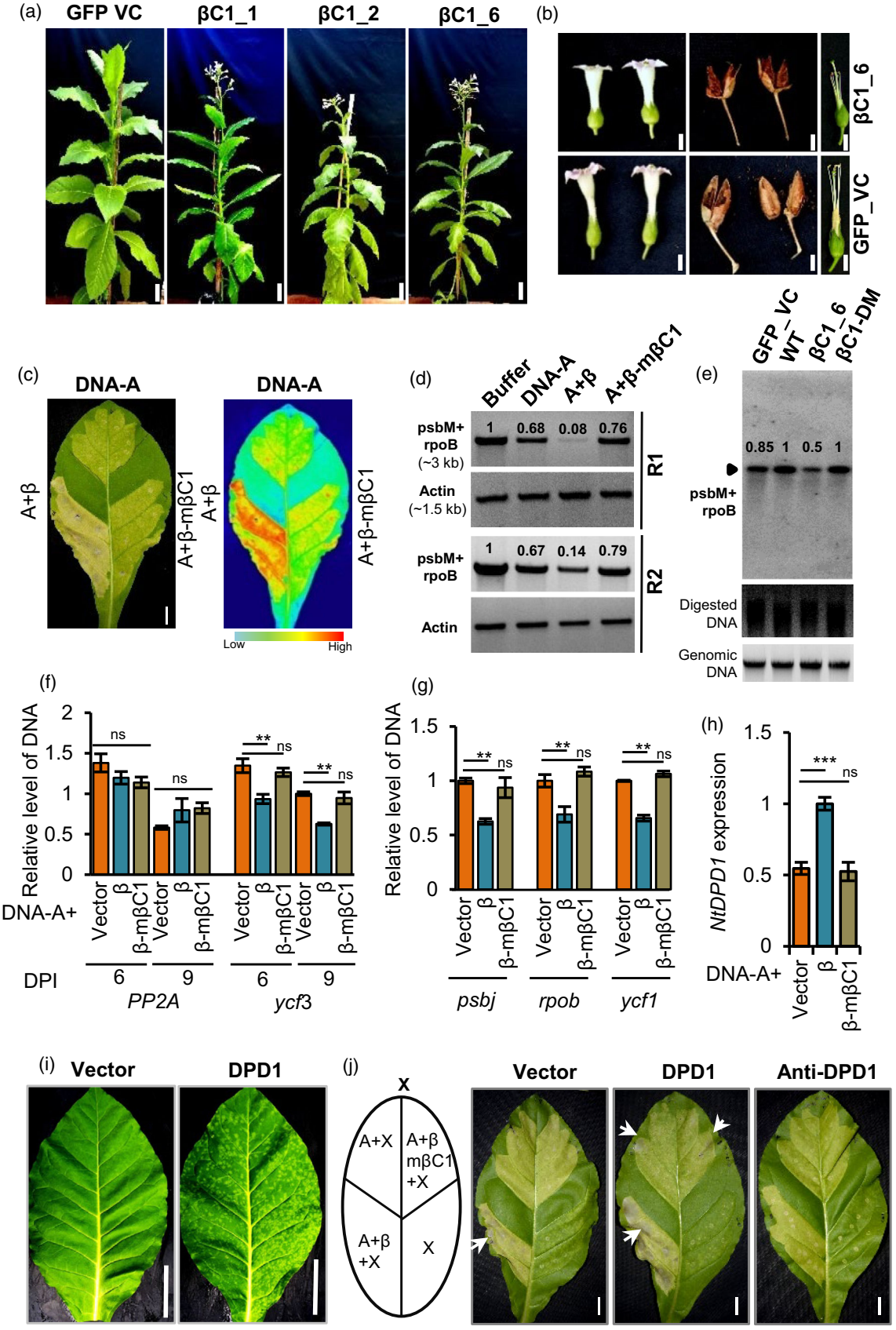

protein was dampened upon C-terminal tagging of the protein with tags (Figure S1a). To understand the cellular pathways affected by βC1, we performed a transcriptome analysis on young leaves of βC1 transgenic plants using the Illumina Hi-Seq platform. We obtained an average of 20 million × 2 paired-end reads for each replicate, of which 92% matched to *Nicotiana tabacum* genome. Upon further characterization of 3576 genes showing maximum differential expression, 1963 genes were found upregulated and 1613 genes were downregulated (Figure S1b,c). Various defense response regulators were found mis-expressed as expected for a pathogenicity determinant protein such as βC1. Innate immune regulators such as secondary metabolite (suberin, lipids, and phenylpropanoid) pathway genes were downregulated in βC1 transgenic plants (Figure S1d). We hypothesized that most of the phenotypes observed in βC1 transgenic plants might be due to disrupted signaling pathways, prominently hormone and circadian rhythm pathways responsible for maintenance of development and vegetative to flowering transition, respectively. In agreement with this, transcripts of GIGANTEA (GI-like) and CONSTANS (CO5-like), key regulators of circadian rhythm, were upregulated 7- and 3.5-fold, respectively, in βC1 transgenic plants. Chlorophyll A/B binding proteins, which are under the control of TIMING OF CHL A/B EXPRESSION1 (TOC1), were upregulated 9.5-fold. A regulator of flowering LATE ELONGATED HYPOCOTYL (LHY) homolog was downregulated six-fold, while its counterpart EARLY FLOWERING 4 (ELF4) was upregulated eight-fold. In addition, multiple auxin-responsive proteins, including YUCA11, were downregulated in these plants, while the cytokinin degrading enzyme CYTOKININ DEHYDROGENASE 7-LIKE was upregulated four-fold (Figure S1e) suggesting deregulation of hormonal signaling in these plants. A similar deregulation of nuclear and plastid genes was observed in chloroplast-localized RALCV βC1 (Bhattacharyya et al., 2015).

Surprisingly, we also observed differential expression of a set of DDR genes involved in genome maintenance and repair in βC1-expressing transgenic plants (Figure S2a). Although previous research suggested deregulation of DDR genes during geminiviral replication (Ascencio-Ibáñez et al., 2008), it was not known which viral protein or proteins might be involved. Interestingly, we observed βC1 expressing transgenic plants showed upregulation of various nuclear encoded DDR genes encoding Rad50-like, photolyases, DRT proteins, BRCA1-like, J-Domain proteins, several nucleases, and helicases (Figure S2a). It is important to note that the majority of the DDR genes that were upregulated in βC1 transgenic plants were necessary for the maintenance of the chloroplast genome (Day & Madesis, 2007). Significantly, multiple nuclear coded but plastid localized proteins such as DRT102, DRT100, DPD1 nuclease, ARC6, and FtsZ, which regulate the copy number, replication, and damage repair of plastid genome, were significantly deregulated in βC1 transgenic plants (Figure S2a). These results indicated a possible plastid genomic subversion leading to the upregulation of nuclear-coded plastid localized DDR response genes in the presence of viral βC1. We also observed modulation of expression for other chloroplast localized genes whose exact role during viral pathogenesis is not clear (Figure S2b,c).

βC1 induces necrosis by destabilizing the plastid genome

Based on phenotype as well as changes in host DDR genes, we hypothesized that the cause for the deregulation of such a huge number of chloroplast genes was likely due to selective plastid DNA destabilization by βC1. Nuclear and chloroplast localized SyYVCV βC1 was previously identified as the causal protein for the symptoms during SyYVCV infection (Nair et al., 2020). We infected *N. tabacum* leaves with SyYVCV DNA-A alone or with DNA-β and DNA-β with point mutations in βC1 open reading frame (DNA-β-mβC1) (mSIM2,3,4; Nair et al., 2020). The point mutations in the SUMO-Interacting Motif (SIM) region of βC1 (mβC1) completely abolished βC1 functions without affecting its chloroplast localization (Nair et al., 2020). Strong necrosis and chlorosis were observed in the segment of leaves infected with DNA-A + β when compared with DNA-A alone (Figure 1c). Furthermore, a very mild chlorosis without noticeable necrosis similar to DNA-A was observed in leaf segments infected with DNA-A + β-mβC1. To check if the stability of the plastid genome was compromised in these leaves, we analyzed abundance and integrity of plastid genome by amplifying a 3-kb segment (*psbM* and *rpoB*) from the plastid genome. A drastic reduction in plastid DNA was observed in the presence of DNA-A + β when compared with control nuclear DNA fragment (Figure 1d). Furthermore, we analyzed the abundance of plastid DNA in βC1 transgenic plants via Southern blotting (SB) analysis. A clear reduction in the plastid DNA in βC1 transgenic plants as compared with vector control or functionally inactive βC1-DM (βC1, C-terminal tagged) plants was observed (Figure 1e). We observed similar reduction in transcript expression upon quantitative real time reverse-transcriptase polymerase chain reaction (real time qRT-PCR) analysis of nuclear and plastid genes (Figure S1f). The degradation of cpDNA, but not nuclear DNA, caused by βC1 was more evident in later stages of infection. These observations were further validated with other plastid genes using DNA qPCR analysis (Figure 1f,g). These results clearly suggest that βC1 selectively destabilizes chloroplastic genome during infection.

Previous studies had highlighted an important role of DPD1 in degrading plastid genome during leaf senescence and pollen development. DPD1 knock-out plants showed preservation of plastid DNA, implicating DPD1 as the nuclease responsible for plastid genome degradation during development (Sakamoto & Takami, 2018; Takami et al., 2018). *DPD1* was upregulated four-fold in our

transcriptome analysis of βC1 transgenic plants (Figure S2a). To confirm this finding, we analyzed the expression of *DPD1* during viral infection and observed a significant induction in the presence of DNA-β, but not in DNA-β-mβC1, confirming that the induction of this nuclease is specific to βC1 (Figure 1h). We further explored a link between βC1-induced necrosis during infection and the induction of DPD1 expression. Necrotic mosaic patches were observed upon overexpression of DPD1 (PVX-*NtDPD1*) in *N. tabacum* and *Nicotiana benthamiana* plants (Figure 1i; Figure S2d,e). This observation was on par with the previous reported function of DPD1 involving nutrient salvage induced necrosis (Takami et al., 2018). To explore further the role of *NtDPD1* in βC1-induced necrosis during viral infection, *DPD1* or antisense-*DPD1* (Full length *DPD1* in antisense orientation to induce knock-down of endogenous *DPD1*) were co-expressed along with DNA-A, DNA-A + β or DNA-β-mβC1 in *N. tabacum* leaves (Figure 1j and Figure S2f,g). As expected, wild-type (WT) βC1 coding DNA-β induced necrosis in vector control leaves (Figure 1j, left panel). The necrosis was considerably enhanced in *DPD1* overexpressing leaves when co-infiltrated along with DNA-β (Figure 1j, middle panel). Interestingly, necrosis was not observed in DNA-β in antisense-*DPD1* expressing leaves (Figure 1j, right panel and Figure S2f). The knock-down of *DPD1* was able to delay virus-induced necrosis to a significant extent as observed at a longer time-point where infected leaves with DNA-β or DNA-β and DPD1-OE exhibited severe necrosis when compared with DNA-β with *DPD-1* knock-down leaves (Figure S2h). These results suggested that plastid DNA was selectively destabilized by βC1-induced DPD1 during viral infection and knock-down of *DPD1* led to reduced virus-induced necrosis.

βC1 induces genotoxicity in bacteria

To gain further insight into the plastid DNA destabilization mediated by βC1, we devised a bacterial cell-based genotoxicity assay. βC1 and its N and C-terminal truncation mutants were expressed in Rosetta-gami (DE3) cells followed by the treatment of a sublethal dose of ultraviolet (UV)C or bleomycin to induce DNA damage (Figure 2a). The UVC dose had minimal to no effect on the viability of cells with active DDR machinery, such as in DE3 protein expressing cells. The control cells expressing maltose-binding protein (MBP) showed appropriate growth before and after induction following stress, suggesting the external sublethal DNA damage was sustained and repaired in these cells. As expected, βC1 expressing cells showed acute lethality, hinting genotoxicity of βC1 in bacteria, similar to plants. βC1δC59 (N-terminal 59 amino acids [AA] expressing truncated form) expressing cells did not show lethality upon induction in UV or bleomycin, whereas βC1δN59 (C-terminal 59 AA) expressing cells showed cell death, similar to full-length βC1. Interestingly, unlike in plants, induction of βC1 caused minimal genotoxicity as seen in the drop assay, while the addition of a sublethal dose of UV along with the induction of βC1-induced cell death. We hypothesized that βC1 by itself is not able to induce complete genotoxicity, but required an additional stress to tip over the balance from damage repair to damage and cell lethality. In plants, virus replication stress might be a tipping point.

To understand the biochemical mechanism responsible for the genotoxicity of βC1, we recombinantly expressed and purified βC1 from *Escherichia coli* using size-exclusion and ion-exchange chromatography. As βC1 from other viruses have been shown to bind to different nucleic acids (Cheng et al., 2011), and the cpDNA was targeted by βC1 in SyYVCV infected plants, we explored if SyYVCV βC1 can bind ssDNA and/or double-stranded (ds) DNA and RNA substrates and if it can alter the stability of nucleic acids. The SyYVCV βC1 was able to bind both ssDNA (Figure 2b) and dsDNA (Figure S3a), but displayed significantly higher binding to ssDNA substrates (Figure 2b). The strength of binding to dsDNA was directly proportional to its length (Figure S3a). However, βC1 did not exhibit significant binding to either ssRNA or dsRNA substrates (Figure S3b–e). We observed significant degradation of ssDNA *in vitro* in the presence of βC1 in multiple biological replicates (Figure 2c). The control MBP protein showed neither binding nor nuclease activity *in vitro*. As nucleases mostly require divalent cations as a cofactor, optimum degradation of ssDNA was detected in the presence of Mg^{2+} ions and to a lesser extent with Mn^{2+} (Figure S3f). We next validated these results using a metal ion chelator EDTA that removes Mg^{2+} from the catalytic interface and did not observe any nuclease activity (Figure 2d; Figure S3g). The ability of βC1 to bind ssDNA was not compromised in the presence of EDTA, suggesting an Mg^{2+} independent DNA binding (Figure 2d). Incubation of purified βC1 with circular ssDNA led to its complete degradation, suggesting that the *in vitro* nuclease activity associated with βC1 has both endonuclease as well as exonuclease activities (Figure 2e). Similar results were observed upon incubation of βC1 with plasmid DNA (Figure S3h). Interestingly, plant DPD1 is also an endonuclease and exonuclease, degrading both ssDNA and dsDNA. Although studies suggest DPD1 is not of endosymbiotic origin, it is likely that βC1 might be regulating other structurally conserved exonuclease family members in bacteria (Sakamoto & Takami, 2018; Takami et al., 2018). Combining all these observations we conclude that *in vitro* purified βC1 has a novel associated nuclease activity that might be involved in cellular genotoxicity.

Specific domains of βC1 mediate genotoxicity, multimerization, and DNA-binding properties

To delineate the motif associated with nuclease activity, we generated multiple point mutants. These point

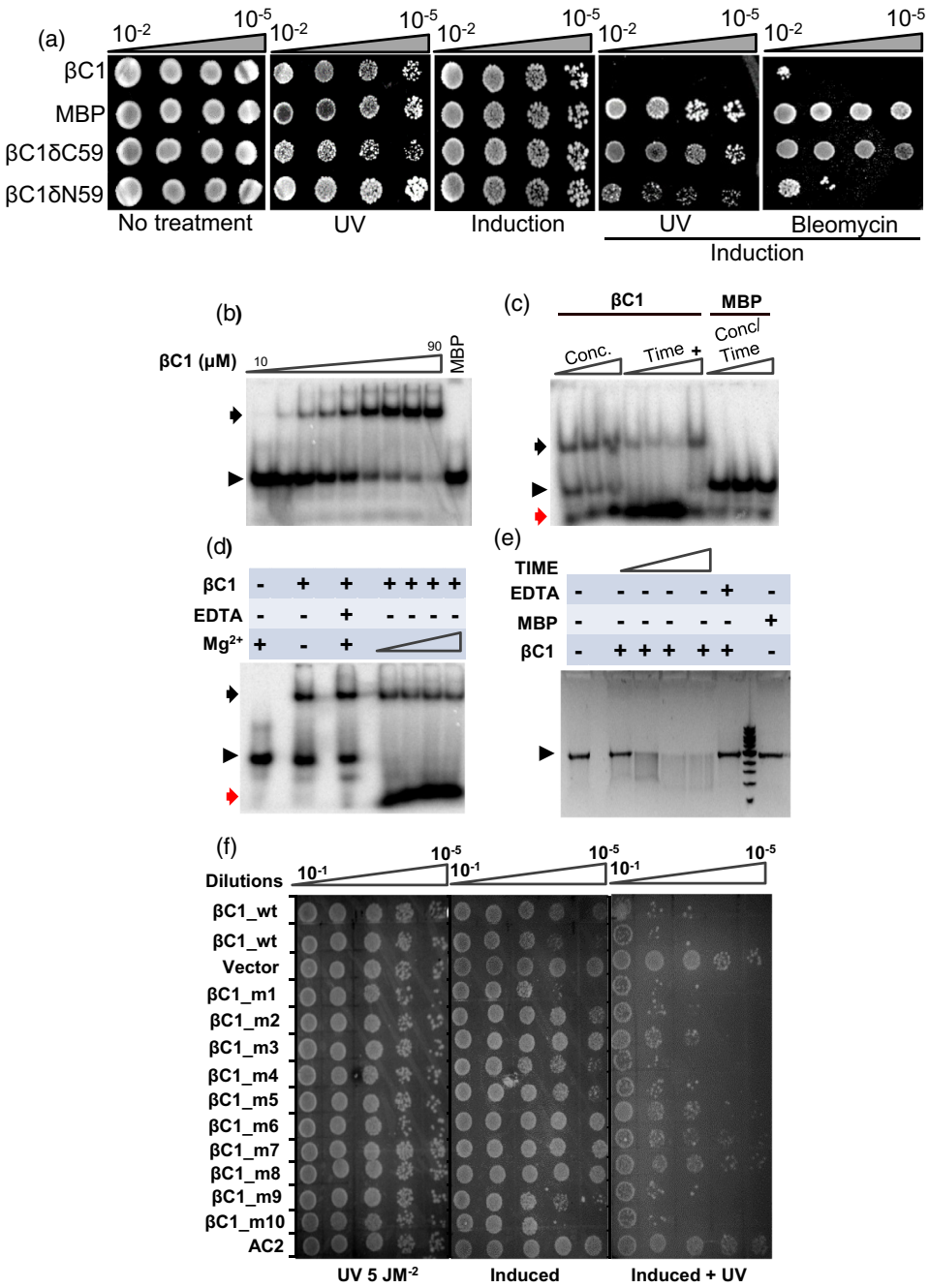

Figure 2. SyYVCV βC1 displays genotoxicity in *Escherichia coli* and associated nuclease activity *in vitro*.
(a) DNA damage sensitivity assay: βC1 was transformed in Rosetta-gami DE3 cells and grown till mid lag phase followed by spotting on LB agar with sublethal ultraviolet (UV): 5 J/m^2, 254 nm. Bleomycin 1 μg ml^{-1}. βC1δC59 and βC1δN59 are βC1 with C-terminal 59 amino acids or N-terminal 59 amino acids truncated (δ), respectively.
(b) Electrophoretic mobility shift assay (EMSA) showing binding of βC1 with single-stranded (ss)DNA in a 8% native polyacrylamide gel electrophoresis (PAGE) gel. Triangle indicates increasing concentration of βC1.
(c) Nuclease assay: βC1 was incubated with ssDNA in various concentrations for varying duration, followed by EMSA in a 6% native PAGE gel. (+) indicates addition of 1 mM EDTA.
(d) Cation dependency assay: Mg^{2+} (1–5 mM) or EDTA (5 mM) was incubated with βC1 and ssDNA followed by EMSA on a 6% native PAGE gel.
(e) Endonuclease activity assay: βC1 was incubated (1–4 h) with covalently closed circular ssDNA (ϕ174) followed by visualization on a 1% agarose gel.
(f) Genotoxicity assay: βC1 and its mutants were spotted on plates in various dilutions and treatments. Induced represents induction of gene with 0.1 mM isopropyl thiogalactose, UV is UVC (254 nm). Figure linked with Figure S3. All assay results were replicated at least three times. Vector expresses MBP. Additional info: N-terminal MBP tagged βC1 (*E. coli* purified, SEC, DEAE) was used in all biochemical assays. MBP parallelly processed with βC1 was used as control. ssDNA substrate used was 49-nt long (150 pg). ssDNA was labeled at 5′ using 32P. Black and red arrows indicate bound and degraded fraction of ssDNA, respectively. Black triangle is unbound substrate.

mutations were made based on their conservation across different βC1 sequences derived from different viruses (Figure S3i). Pairwise sequence identity among 25 different βC1 sequences from various viruses was 45.6%. A detailed analysis of the alignment pointed to a few conserved residues that were mutated to obtain various βC1 mutants (mutants 1–10) (Figure S3j). All mutants were recombinantly purified with methods similar to WT βC1 (Figure S3k), and their DNA binding ability was analyzed along with WT βC1 as a positive control. MBP acted as a negative control. While controls behaved as expected, mutants 6 and 8 showed significant reduction in binding to ssDNA (Figure S3l). None of these point mutations completely abolished the observed nuclease activity. However, we observed a reduction in the nuclease activity in mutants 6, 7, and 8 (Figure S3m).

To delineate the genotoxicity domain of βC1 further, we used cell-based UV-genotoxicity assay. We used MBP and SyYVCV AC2, another nucleic acid-binding protein of SyYVCV (Sung & Coutts, 1996), as controls. As expected, βC1 expressing cells showed acute lethality after sublethal UV stress. A few βC1 mutants (mutants 10 and 1) showed enhanced lethality during induction as well as with UV stress when compared with WT βC1. Fascinatingly, mutants 7, 8, and 6 showed a significant decrease in cell lethality (Figure 2f). MBP and AC2 expressing cells showed appropriate growth before and after induction following stress. These results reinforced our previous observation that βC1-associated nuclease activity was capable of causing genotoxicity in cells and its C-terminus domain is involved in this activity.

βC1 exists as multimers *in vivo* as well as in purified fractions (Cheng et al., 2011). Multimerization might influence the DNA binding of proteins. We recombinantly expressed and purified βC1 in *E. coli* and observed higher-order multimers as well as monomers in a size-exclusion analysis (Figure 3a). To delineate the multimerization motif, we generated various truncation mutants of βC1. WT βC1 protein eluted just after the void volume on the contrary to its predicted elution peak just before the purified MBP tag, suggesting that βC1 protein (MBP-βC1, approximately 59 kDa) formed multimers (>650 kDa) in solution (Figure 3a). All the truncation mutants of βC1 except δN59 were able to form multimers. Careful examination of the truncation mutants fine mapped the minimum multimerization domain between residues 51 and 59 (Figure 3b; Figures S3i and S4a–l). The δC59 showed multimerization similar to WT βC1, whereas in δN59, the multimerization activity was completely abolished (Figure 3c). Interestingly, the DNA-binding ability of the δN59 mutant was significantly reduced when compared with other mutants (Figure 3d,e), suggesting that multimerization and DNA binding domains overlap. The C-terminus is essential for observed genotoxicity in bacteria (Figure 2a), but the DNA binding domain is mostly localized in the N-terminus (Figure 3d). These results suggests that βC1 C-terminus can indirectly induce genotoxicity, likely by inducing nucleases in bacteria.

βC1 expressing bacterial cells require RecA for survival

In *in-vitro* DNA binding assays, purified βC1 had associated nuclease activity whereas in bacterial cells, the genotoxicity was conditional. RecA family of proteins maintain the integrity of bacterial genome and its homologs are conserved in chloroplast genome (Maslowska et al., 2019; Rowan et al., 2010). In bacterial cells, RecA protein acts as the central regulator of DDR machinery. We hypothesized a direct role of RecA in DNA damage response induced by βC1. We used BLR (DE3) cells that lack a functional RecA protein in genotoxic assay. MBP control or empty vector did not show any difference in growth among treatments; however, as expected, βC1 expressing cells did not survive the induction in BLR (DE3) (Figure S5a,b). We tested the effect of βC1 mutants in BLR cells and observed that mutants 7, 8, and mβC1 rescued cells from lethality, reinforcing results observed in the UV assay, and highlighting the role of C-terminal in genotoxicity (Figure 2f; Figure S5c). The mβC1 mutant used in this assay was the same as that used in β-mβC1 for *in vivo* assays.

To verify the role of RecA, we complemented *Caulobacter vibrioides RecA* (Cv*RecA*) in βC1 expressing BLR (DE3) cells. The *CvRecA* protein is a close homolog of *E. coli RecA* (*EcRecA*), and this complementation completely abrogated βC1-induced genotoxicity (Figure S5d). These results suggest that RecA is required by bacterial cells to subdue βC1-induced genotoxicity.

We used truncation mutants of βC1 to delineate the minimum motif required for genotoxic effects in bacteria by employing both UV stress and BLR (DE3) based assays. Interestingly, truncating even as a minimum of eight residues (δC8) from the C-terminus significantly altered the genotoxic activity of βC1 (Figure 4a). Careful examination of the results showed a complete loss of lethality upon truncating 42 residues (δC42) from the C-terminal. Surprisingly, we observed an increase in genotoxicity in N-terminal truncation mutants δN20 and δN21-51 of βC1 (Figure 4a–c). Similar results were also observed in point mutants of βC1 (mutant 10) that has substitutions in the N-terminal 20 residues (Figure 2f). These results suggested that the C-terminal of βC1 induces genotoxicity in cells while its N-terminus might be essential for regulating this activity.

Bacterial RecA physically interacts with begomoviral βC1

It was previously observed that virulence proteins such as the pathogenicity determinants (for example, Rep protein) interacted with Rad proteins (Kaliappan et al., 2012). βC1 BLR (DE3) genotoxicity assay further hinted to a direct role

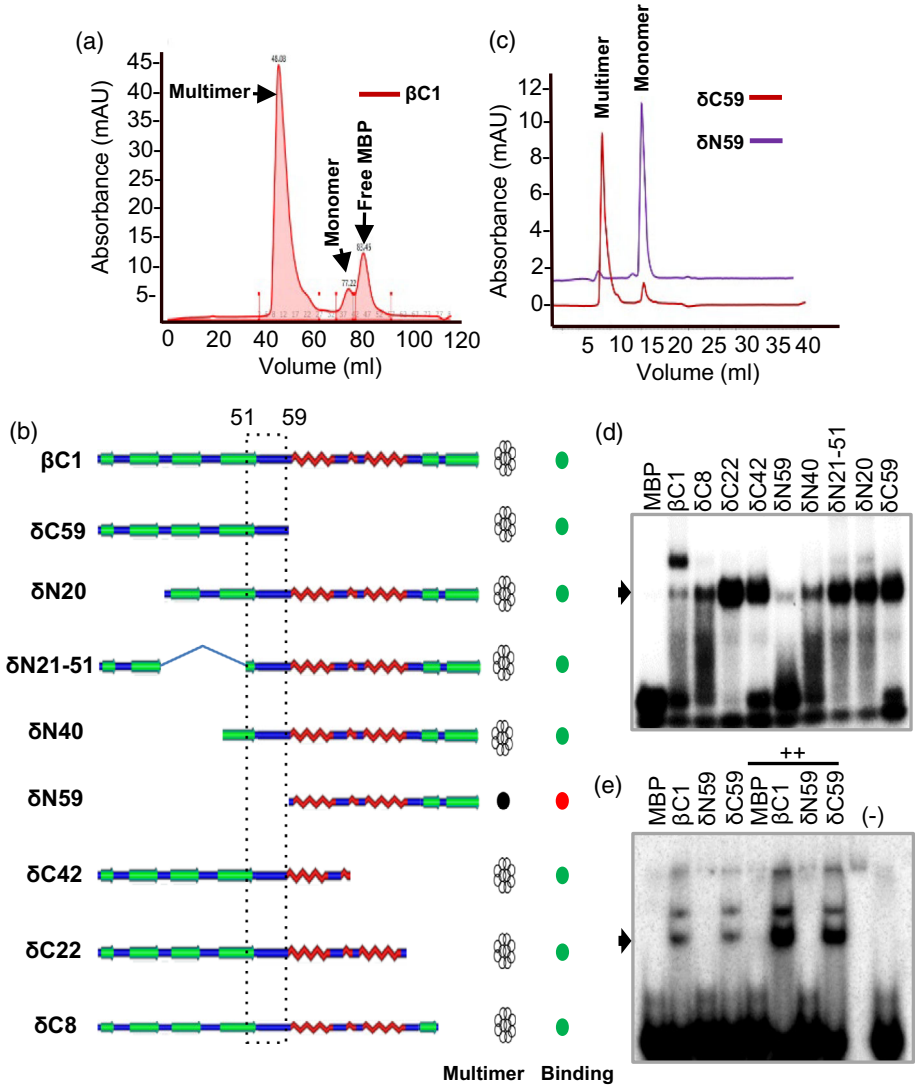

Figure 3. Demarcation of multimerization domain of βC1.
(a) Size exclusion profile of maltose-binding protein (MBP)-βC1 on a SD200 preparative column highlighting multimer, monomer, and free MBP in βC1 fractions.
(b) Schematics of βC1 truncation mutants showing a summary of size exclusion analysis in a SD200 Sephadex analytical column. Right side columns depict multimerization and DNA binding state of respective protein. Green and red circles indicate presence or absence of DNA binding, respectively. Schematic is based on size-exclusion profiles shown in Figure S4.
(c) Overlaid size exclusion profile of C-terminal (δN59) and N-terminal (δC59) truncation mutants of βC1 analyzed on an SD200 analytical column.
(d) Electrophoretic mobility shift assay showing single-stranded DNA binding of βC1 and its truncation mutants.
(e) Same as (d) except N and C terminal truncation mutants were used. ++, two-fold increase in protein; (−), no protein controls; black arrow, binding.

of RecA in modulating activity of βC1. Using RecA-specific antibody, we were able to detect RecA in purified βC1 fractions. A 37-kDa band was detected in the purified βC1 protein fraction but not in the MBP fraction. Interestingly, RecA interaction was detected in the C-terminus truncation mutant (δC59) of βC1 but not in the N-terminus truncation mutant (Figure 5a).

To verify the interaction of βC1 and RecA further, we performed an *in vitro* pull-down assay (Figure S6a) using 6X-HIS-*Cv*RecA. βC1, but not MBP, bound to *Cv*RecA, suggesting that βC1 can selectively bind to RecA. The DNase I-treated βC1 sample was also able to pull-down RecA, suggesting that the interaction of βC1 with RecA is not through shared affinity for DNA (Figure S6a). We further confirmed that the interaction of βC1 with RecA by affinity purification mass spectrometry (MS) (Table S1). RecA along with its other DDR counterparts such as RecBCD, dnaJ, and dnaK were identified with high scores in affinity purification MS. Interestingly, nucleases such as exonuclease-7 and SbcCD nuclease were also detected, reinforcing our previous observation of associated nuclease activity. These results suggest that RecA can physically interact with βC1 and is

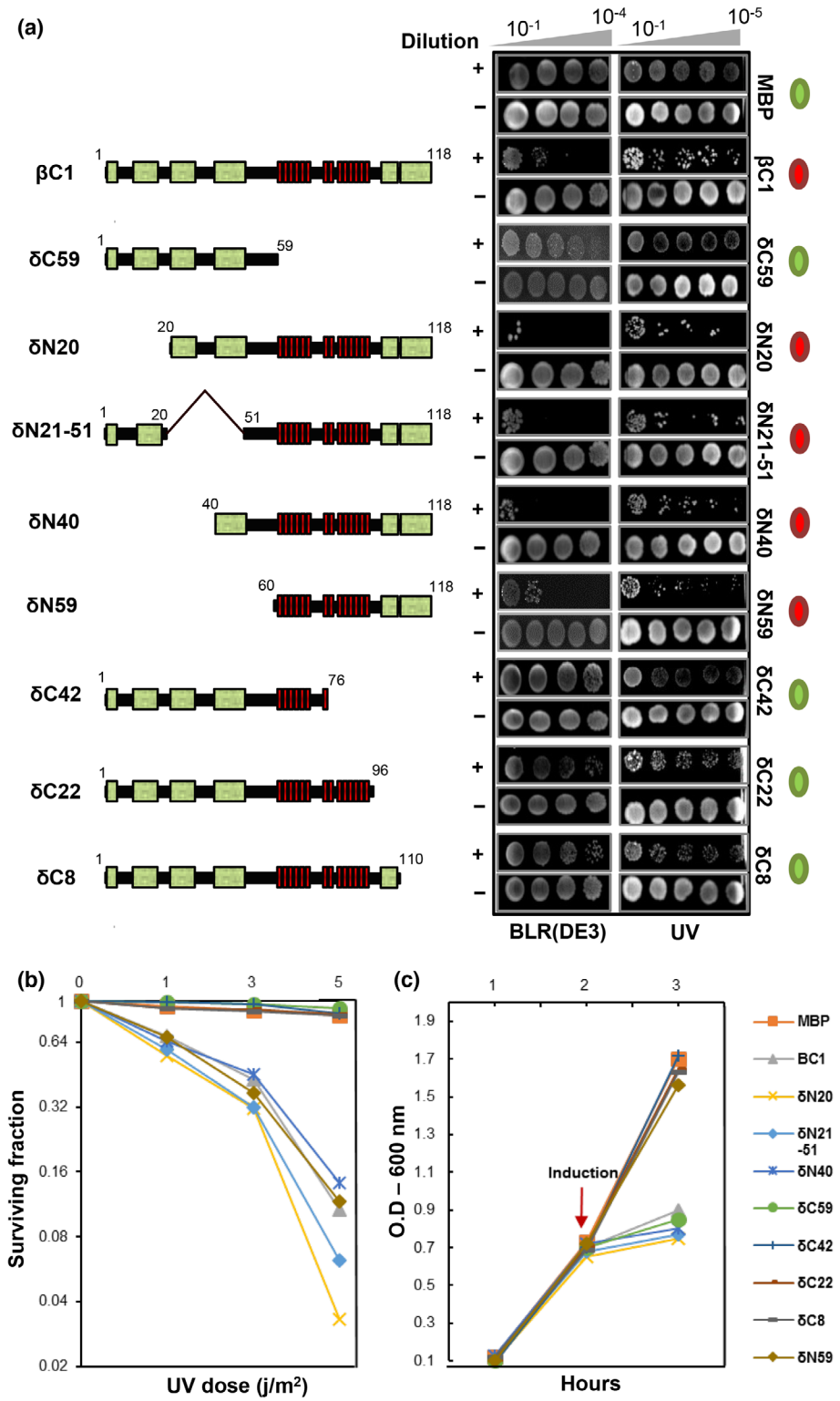

Figure 4. SyYVCV βC1 C-terminal end is required for inducing genotoxicity.
(a) Schematic diagram of βC1 mutants (left panel). βC1 and its mutants were transformed in BLR (DE3) cells and induced with isopropyl thiogalactose (middle panel). Right panel: βC1 was expressed in Rosetta-gami cells followed by spotting and exposure to ultraviolet (UV)C. MBP, maltose-binding protein.
(b,c) Plots showing survival rate and growth after (b) UV treatment and (c) induction of βC1 in BLR cells (0.2 mM), respectively. Green and red circles represent majority fraction of cells being alive or dead.

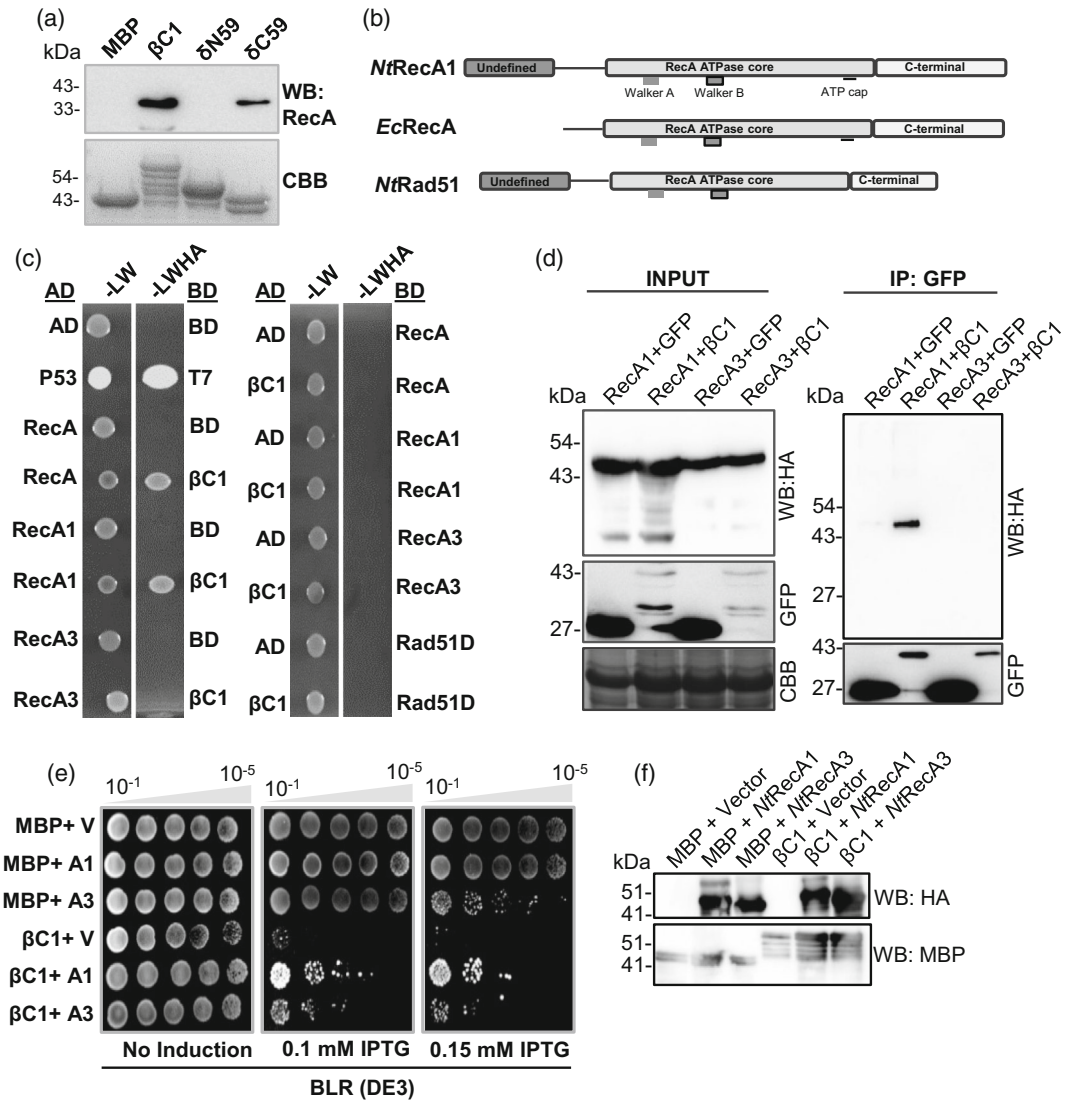

Figure 5. *Nt*RecA1 interacts with SyYVCV βC1.
(a) Western blot (WB) of purified βC1 with anti-RecA indicating the presence of *Ec*RecA in purified βC1 fractions, $n = 3$. MBP, maltose-binding protein.
(b) Domain architecture of RecA and its plant homologs.
(c) Yeast two-hybrid assay showing interaction of βC1 with RecA and its plant homologs. Dilution shown is 10^{-2}. Assay was performed with different dilutions and knockout media. Representative image shown. AD, activation domain; BD, binding domain. Synthetic double-knockout media lacking leucine and tryptophan (-LW) was used for selection of transformants. Quadruple-knockout medium lacking leucine, tryptophan, histidine and adenine (-LWHA) was used to screen for interaction.
(d) *in planta* pull-down assay to check interaction of βC1 with RecA homologs. RecA homologs were tagged with hemagglutinin tag (HA) and βC1 was tagged with green fluorescent protein (GFP). GFP was taken as control.
(e) Complementation of *Nt*RecA1 (A1), *Nt*RecA3 (A3) or vector (pet22b+, V) in MBP or βC1 expressing BLR (DE3) (recA$^-$) cells. IPTG, isopropyl thiogalactose.
(f) WB confirmation of complementation experiment. RecA1 and RecA3 were tagged with HA and βC1 with MBP. RecA1 and RecA3 protein size: approximately 45 kDa, βC1: approximately 59 kDa, MBP: approximately 42 kDa.

co-purified with βC1 during its recombinant expression in *E. coli*.

RecA1, a plant homolog of bacterial RecA, can interact with βC1 *in planta*

RecA has close homologs across all walks of life. We wondered if such an interaction is possible in host plants with functional consequences. RecA1 and RecA3 are the closest plant homologs of bacterial RecA. RecA1 is exclusively chloroplastic with an AA sequence similarity of 64%, whereas RecA3 is mitochondrial and 66% similar to *EcRecA* (Cerutti et al., 1992; Khazi et al., 2003; Rowan et al., 2010) (Figure 5b; Figure S6b). We used a yeast two-hybrid (Y2H) system to identify if βC1 interacts with plant RecA homologs (Figure 5c; Figure S6c). As expected, RecA exhibited strong interaction with βC1 in quadruple

knockout media. We did not observe any interaction of Rad51D with βC1 in our Y2H screen (Figure 5c). Among the plant homologs, *Nt*RecA1 exhibited strong interaction with βC1 while other homologs were unable to interact with it.

To validate the Y2H results and to verify RecA1 interaction with βC1 *in planta*, we employed an *in planta* pull-down assay (Figure 5d). Both *Nt*RecA1 and *Nt*RecA3 were tagged with hemagglutinin tag (HA) and co-expressed with GFP-βC1. We detected interaction for *Nt*RecA1 in the pull-down assay but not *Nt*RecA3, suggesting that βC1 interacts specifically with *Nt*RecA1 (Figure 5d). NtRecA1 has been shown to possess exclusive plastid localization. Our previous study (Nair et al., 2020) showed that βC1 has both nuclear and plastid localization property. It is very likely that βC1 is interacting with RecA1 in the chloroplast.

As complementing *Cv*RecA in BLR (DE3) expressing βC1 cells significantly reduced cell lethality, we tested whether the plant homolog of *EcRecA*, *NtRecA1*, which interacted with βC1 *in planta*, can complement BLR (DE3)::βC1 cells (Figure 5e). BLR (DE3)::βC1 cells as expected were not viable, but upon complementation with plant RecA1 showed a significant increase in cell viability. *Nt*RecA3 was able to complement βC1 only weakly (Figure 5e). All proteins expressed appropriately in the complemented system (Figure 5f). Together, these results suggested that βC1 can interact with RecA homologs in plants and such an interaction has conserved function as plant RecA1 was sufficient to alleviate βC1 induced genotoxicity in bacteria.

DNA binding property of plant RecA1 is modulated by βC1

RecA1 is essential for maintaining the genetic stability of cpDNA. Binding of βC1 to *Nt*RecA1 might alter the activity of RecA1. *Nt*RecA1 was able to bind specifically to both ssDNA and dsDNA probes (Figure 6a,b; Figure S7a). Similarly, *Ec*RecA bound to both forms of DNA (Figure S7b). We hypothesized that the DNA-binding property of RecA might be altered in the presence of βC1. As SyYVCV βC1 has a strong affinity to ssDNA and rather a weak binding to dsDNA of smaller length, the assay was designed to probe the ability of RecA to bind dsDNA in the presence of WT βC1 or its truncation mutants. Interestingly, dsDNA binding of RecA was significantly altered with βC1

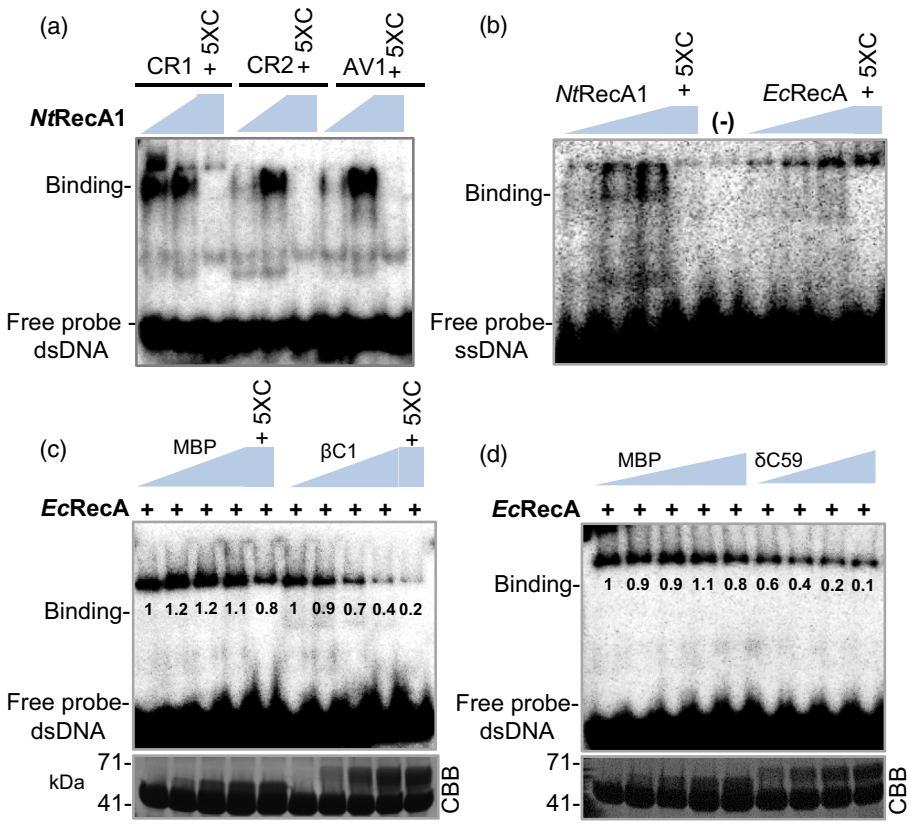

Figure 6. βC1 modulates DNA binding property of RecA.
(a) Gel shift assay showing interaction of *Nt*RecA1 with dsDNA probes.
(b) Same as (a) except ssDNA probes.
(c,d) Electrophoretic mobility shift assay competition assay: RecA protein was co-incubated with viral DNA probe along with varied concentrations of maltose-binding protein (MBP)-βC1, βC1 truncation mutant or MBP alone, before resolving. Coomassie Brilliant Blue (CBB) shows amount of total protein. CR1, CR2, and AV1 fragments are 40 bp long DNA oligos with sequence of SyYVCV CR1, CR2, and AV1 regions as indicated in Figure S7a. 5XC represents five-fold molar excess of competitive inhibitor (cold probe). MBP-βC1: 59 kDa, MBP: 42 kDa, RecA: 38 kDa.

(Figure 6c). As shown earlier, the N-terminal half of βC1 was responsible for binding to RecA. Titrating (δC59) N-terminal half of βC1 protein with RecA reduced binding (Figure 6d), whereas, C-terminal half of βC1 (δN59) did not alter the DNA binding property of RecA (Figure S7c). These results suggest that interaction of βC1 with NtRecA1 alters the dsDNA-binding ability of the latter.

*Nt*RecA1 augments viral replication in host plants

We tested whether the interaction of βC1 with *Nt*RecA1 alters viral replication by performing a viral replication assay (Figure 7a). p35S::*Nt*RecA1-HA and GFP-βC1 were co-infiltrated along with SyYVCV DNA-A in *N. benthamiana* and *N. tabacum*. Viral RFs were analyzed using SB in three independent replicate experiments. As controls, p35S::GFP was used along with an empty vector. As expected and previously observed (Nair et al., 2020), βC1 enhanced the viral titer (Figure 7a). The accumulation of viral replicons increased in the presence of *Nt*RecA1 and WT βC1, but not with βC1-DM mutant. qPCR analysis of the Rep (C1) region also suggested an additive effect of *Nt*RecA1 in the presence of βC1 but not with βC1-DM (C-terminal tagged βC1, functionally inactive) (Figure 7b). We also performed a similar experiment in *N. tabacum* where we used *Nt*RecA1 and *Nt*RecA3 in a time-course analysis of viral replication (Figure S8a). Viral SyYVCV DNA-A replication was higher in all the time points in the presence of *Nt*RecA1 but not with *Nt*RecA3 (Figure S8a,b). These results suggest that the interaction of βC1 with RecA1 is beneficial for viral replication.

RecA1 enhances βC1-derived viral symptoms

βC1 is responsible for chloroplastic DNA degradation and chlorosis during infection (Figure 1). To analyze the function of its interaction with RecA1, we infected DNA-A or DNA-A + β in combination with PVX-RecA1 or PVX-antisense-RecA1 (anti-RecA1, full length NtRecA1 in antisense orientation to induce knock-down of endogenous RecA1 (Figure 7c; Figure S8e) in *N. tabacum* leaves. There was no difference observed in DNA-A-induced symptoms in the presence of either *Nt*RecA1 or anti-*Nt*RecA1 (Figure 7c, left panel). Interestingly, we observed an increase in chlorosis and the large necrotic areas in DNA-A + β inoculated leaves when co-infected with *Nt*RecA1 when compared with anti-RecA1 (Figure 7c, middle panel and Figure 7e). This result is in agreement with the results of the viral replication assay. Neither *Nt*RecA1 nor anti-*Nt*RecA1 produced any chlorosis or necrosis when expressed alone (Figure 7c, right panel and Figure S8c), suggesting that *Nt*RecA1 can only augment symptom determinant function of βC1. Correspondingly, we observed an increase in the PVX-βC1 symptoms upon co-infection with RecA1 as compared with antisense-*Nt*RecA1 (Figure S8c,d). In addition, large necrotic spots were observed in DNA-A + β but not in DNA-A + βmβC1 in the presence of *Nt*RecA1 (Figure 7d,f). Interestingly, DPD1 expression was upregulated in presence of WT βC1 irrespective of *Nt*RecA1 (Figure S8f). These results suggest that RecA1 directly or indirectly increases viral symptoms in the presence of DNA-β coding for βC1.

DISCUSSION

A mature plant cell contains hundreds of chloroplasts. Each chloroplast contains a relatively small-sized genome (cpDNA; 100–200 kb) in multiple copies (Day & Madesis, 2007; Sakamoto & Takami, 2018; Sato et al., 2003). In tobacco, Arabidopsis and in maize, cpDNA remains relatively stable until senescence (Golczyk et al., 2014). The high copy number of cpDNA is essential for adequate rRNA production required to sustain the arduous photosynthetic apparatus (Bendich, 1987; Udy et al., 2012). Subunits of important photosynthetic enzymes are not abundant when compared with the cpDNA-coded mRNAs, suggesting the role of translational machinery as a checkpoint for chloroplastic efficiency (Eberhard et al., 2002; Hosler et al., 1989). The relatively constant and high copy

Figure 7. RecA1 augments pathogenicity determinant function of βC1.
(a) Viral replication assay with SyYVCV DNA-A partial dimer co-inoculated with NtRecA1, βC1 or both, in *Nicotiana benthamiana*. Southern blot was performed at 7 days post-inoculation using full length DNA-A probe. One replicate Southern blot is shown.
(b) Same as (a) except quantitative polymerase chain reaction of viral Rep gene transcripts. NPTII was used as internal control. Histogram represents data from three biological replicates, each with three quantitative polymerase chain reaction technical replicates.
(c) RecA1 or anti-RecA1 infiltrated either alone or with DNA-A and DNA-A + β in *N. tabacum* leaves. $N = 3$.
(d) Same as (c) except DNA-βmβC1 was co-infiltrated along with RecA1 and anti-RecA1.
(e,f) Quantification of the necrosis observed in infected leaves in (c) and (d), respectively. Quantification of necrotic area was done using FIJI. Scale bar, 2 cm. Images were taken at 12 days post-inoculation. (b,e,f) Ordinary one-way ANOVA Dunnett's multiple comparison test, $^{***}P \leq 0.001$ and $^{****}P \leq 0.0001$. ns, not significant.
(g) Summary (left panel) (SyYVCV DNA-A alone infected plants): RecA1 maintains the multicopy plastid genome allowing normal metabolic output for the cell. During virus infection, pathogenic signal is relayed to chloroplast causing release of Ca^{2+} from thylakoids into the stroma. Increased stromal Ca^{2+} leads to the increase in $^1O_2$ and other ROS species, which are the key molecules for retrograde signaling between nucleus and chloroplast. This leads to transcription and translocation of nuclear defense responsive genes into the chloroplast followed by enhanced synthesis of hormones and secondary metabolites. Viral movement and replication is severely curtailed due to plastid mediated defense, reducing symptom severity and disease. Right panel (DNA-A + β infected plants): in the presence of SyYVCV βC1, plastid genome maintainer RecA1 is recruited and forms a complex with βC1. Simultaneously, βC1 upregulates plastid nuclease DPD1 to destabilize plastid genome, reducing the photosynthetic output and capability to code for key enzymes synthesizing defense moieties. Parallelly, in the presence of βC1, degradation of plastid genome by induction of DPD1, releases enormous pool of inorganic phosphate into the cytoplasm. Phosphate is a key limiting element for nucleic acid synthesis that might boost viral replication.

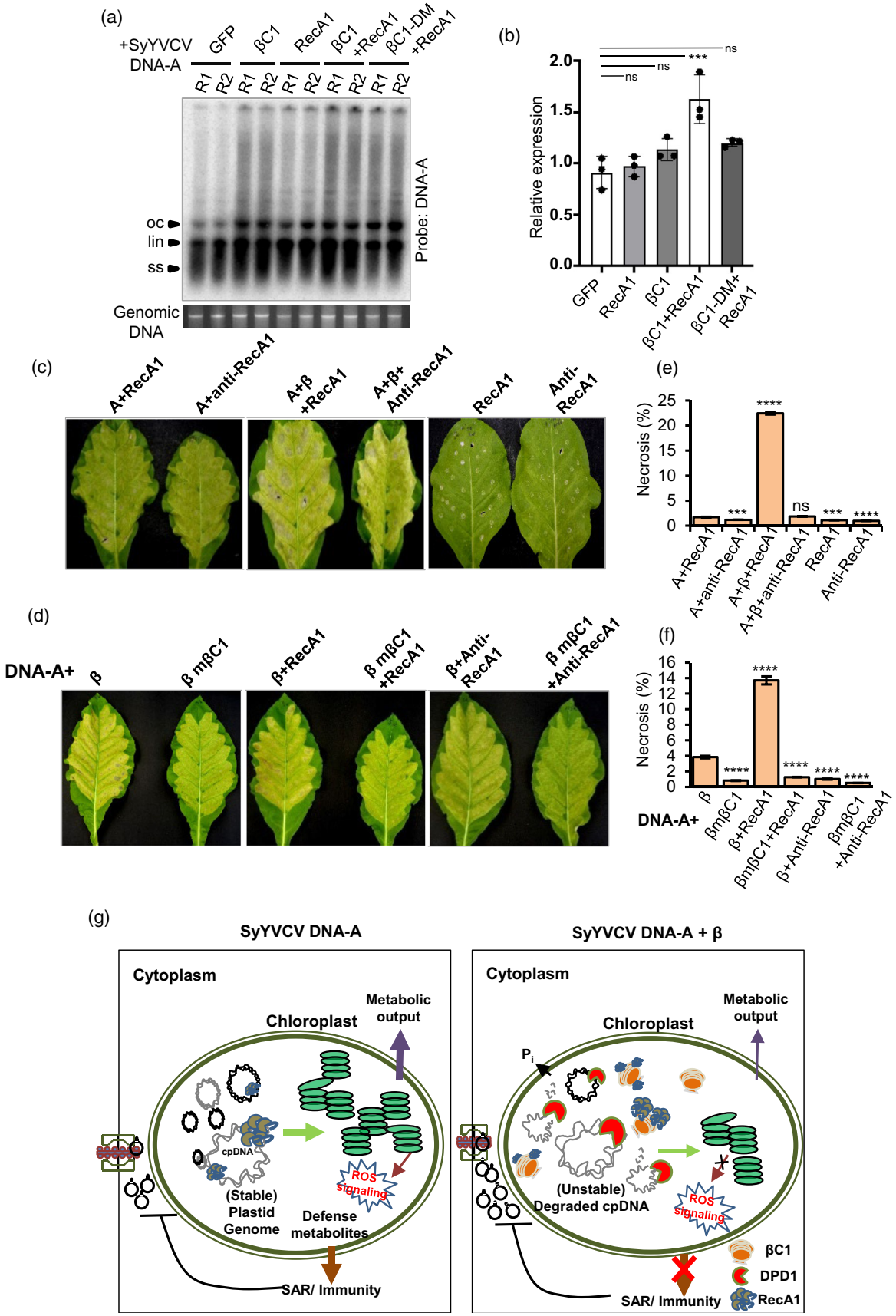

number of cpDNA is maintained by nucleoid-dedicated replication repair and organization proteins. Homologs of bacterial RecA proteins are crucial for the maintenance of the organellar genome in higher organisms. RecA homologs, particularly RecA1, forms complex with various DDR members to maintain the integrity of the plastid genome (Inouye et al., 2008; Odahara et al., 2017; Odahara, Inouye, et al., 2015; Odahara, Masuda, et al., 2015). Arabidopsis cp*recA* mutant lines had a drastic effect on the organelle function due to loss of genomic integrity and uncontrolled recombination in cpDNA (Rowan et al., 2010).

The cellular repair pathway plays an important role in maintaining the integrity of the nuclear as well as organellar genome (Kunkel, 2004). Considering these evidences, it is also likely that interaction of βC1 with RecA1 might directly involve the DDR complex in the replication and repair of virus RFs, guiding cellular machinery to viral replisomes in the host nucleus. In fact, our results showed an increase in viral replication and symptoms upon RecA1 overexpression only in the presence of βC1.

The ability of βC1 to induce genomic instability was due to its DNA-binding ability and an associated nuclease activity, the latter due to its nuclease partners. βC1-associated nuclease activity led to the induction of genotoxic stress in bacterial and plant cells (Figure 2). The genotoxic activity of βC1 in *E. coli* can be extrapolated to its role during plant infection, where plastid DNA degradation and cell death are associated with its expression. The additional sublethal stress was essential for tipping the balance of repair and damage in the genotoxicity assay in *E. coli* cells, whereas, in plants, replicating virus might act as the additional stress. Based on our observations, βC1 appears directly to modulate the function of RecA1 and possibly redirects RecA1 for virus replication. Simultaneously, βC1 induced a plastid specific nuclease, DPD1, to initiate cpDNA degradation. It appears that βC1 might divert RecA1 from maintaining the plastid genome.

We hypothesize two functions of the plastid genome subversion activity of βC1. The reduction in plastid genome results in decreased coding capacity, significantly altering its antiviral response-ability. Consequently, SA-induced PATHOGENESIS RELATED GENE (PR) expression is severely repressed. SA is synthesized in chloroplast and is regulated by plastid retrograde signaling mediated by ROS. βC1 selectively disrupted plastid signaling, downregulating ROS, as was evident in βC1 transgenic plants. The mβC1 without genotoxic activity neither affected plastid DNA nor was it able to repress PR gene expression (Figure S8g,h). Alternatively, as the *Begomovirus* infects differentiated cells, availability of raw materials for replication is limited. Degradation of the plastid genome by DPD1 might be a common mechanism to cope with phosphate deprivation (Takami et al., 2018) and active salvage pathway (Tang & Sakamoto, 2011). Nucleic acids and phospholipids are the most abundant source of phosphorous esters. Multiple copies of the organellar genome can encrypt massive storage of phosphate that a virus might exploit during replication. In accordance with the hypothesis, along with DPD1, we also observed significant upregulation of bifunctional nuclease (BFN1) that are well characterized for their role in salvaging RNA during senescence (Figure S2a) (Pérez-Amador et al., 2000). The destablization of chloroplast genome that we have demonstrated here might also have contributions from the virus infection itself and discerning this needs further elaborate studies. Organellar DNA serves as a "dispensable" phosphate source that can be readily tapped into without significantly disturbing the cellular homeostasis. Nutrient stress leads to reduction in organellar DNA and relocation of vital minerals, similar scenario should also exist in cell-cycle exited cells during viral replication. Such possibilities are interesting and might be of future interest in other plant–pathogen interactions. It is worth mentioning that most plant pathogens induce chlorosis and necrosis in susceptible host plants and might share similar mechanisms.

EXPERIMENTAL PROCEDURES

Plasmids and cloning

Cloning was performed as previously described (Nair et al., 2020). Briefly, the partial dimer of DNA-A and DNA-β was amplified from pSD30 and pSD35, respectively, and cloned into pBIN19 using *Bam*HI and *Sac*I sites (Das et al., 2018). For plant transformation and transient expression, βC1 and RecA proteins were cloned into modified pBIN19 (35S CAMV promoter) vectors using *Bam*HI and *Sac*I sites for βC1, and *Bam*HI and *Xho*I for RecA proteins. For βC1 fusion constructs, βC1 was amplified using primers AN34 and AN35 containing *Sal*I and *Sac*I (Table S2). eGFP was amplified from pMEL2 (pBIN HSP30-eGFP) using primer pair AN30 and AN31 having *Bam*HI and *Sal*I along with a short linker sequence (Gly-Gly-Ser-Gly). The vector pBIN-GFP was digested with *Bam*HI and *Sac*I to release approximately 700-bp product. βC1 amplicon was digested with *Sal*I and *Sac*I and eGFP amplicon was digested with *Bam*HI and *Sal*I. A three-fragment ligation was performed using βC1 fragment, eGFP fragment, and linearized vector. For recombinant protein purification vectors, βC1 (insert) was amplified from pAN3 using primer pair AN3 and AN4 containing *Kpn*I, precision protease cleavage site (Leu Glu Val Leu Phe Gln/Gly Pro) in AN3 and *Xho*I, *Not*I sites in AN4. pMAL-p5E vector and βC1 were digested with *Kpn*I and *Not*I. Primer and plasmid used in the study are detailed in (Tables S2–S4).

Recombinant protein purification

For protein purification, Bl21 (DE3) or Rosetta-gami (DE3) (Novagen) cells were typically used unless otherwise mentioned. For purification of βC1 and its mutants, cells were grown to OD 0.7 at 37°C and induced with 0.3 mM isopropyl thiogalactose at 20°C. The induced culture was incubated with shaking at 16°C for 18 h. The cells were pelleted and lysed using sonication (10 sec on and off for 15 cycles, 60% amplitude) in the lysis buffer (50 mM Tris-Cl pH 8, 500 mM NaCl, 5% glycerol, 5 mM 2-mercaptoethanol, Igepal 0.01%, and protease inhibitor tablets; Roche). The lysate was clarified using centrifugation and the supernatant was passed through

pre-equilibrated dextrin-Sepharose beads (GE). The purified protein was then passed through a Q-Sepharose (ion-exchange column; GE) and protein was eluted using NaCl gradient. The ion-exchanged purified protein was further concentrated and passed through a size-exclusion column (SD-200, HiLoad 16/600 200 pg Superdex preparative column; GE) and the protein fraction was concentrated and stored in storage buffer (25 mM Tris-Cl pH 8, 100 mM NaCl, 5% glycerol) at −80°C.

Transgenic plants and transient expression

Transformation of tobacco (*N. tabacum*, Wisconsin 35) was performed as described previously (Nair et al., 2020; Sunilkumar et al., 1999).

RNA-sequencing analysis

RNA-sequencing (RNA-Seq) analysis was done as previously described (Jha et al., 2021). Paired-end (100 × 2) RNA-Seq reads were adapter trimmed using CUTADAPT (Martin, 2011) and aligned to the genome (*N. tabacum*: TN-90) using HISAT2 (Kim et al., 2019). Differentially expressed genes were identified using CUFFDIFF with log2 fold-change >1.5 (Trapnell et al., 2011), and Gene Ontology analysis was performed using PANTHER (Mi et al., 2021).

Plant growth conditions

For phenotyping of plants, 2-week-old rooted plants grown in rooting media were transferred to soil and kept in a controlled environment (growth chamber, temperature: 24°C, light setting 4 (panasonic MLR-352 growth chamber) with 12 h cycle and relative humidity 70%) for 1 week to acclimatize. Hardened plants were further transferred to larger pots in a transgenic greenhouse (temperature: 24°C, relative humidity 70–80%, and natural light cycle).

Plant total protein isolation and western blotting

Total protein was isolated using the acetone-phenol extraction method and western blotting was performed as previously shown (Nair et al., 2020; Wang et al., 2006). Antibodies used in this study are listed in Table S5.

Immunoprecipitation

Immunoprecipitation was performed as previously described (Nair et al., 2020). Briefly, infiltrated or transgenic plant leaves expressing the protein of interest were finely powdered under liquid nitrogen. Three volumes of lysis buffer (50 mM Tris-Cl pH 7.4, 150 mM KCl, 1% Triton-X100, Protease inhibitor 1 X [Roche], NEM 20 μM) was added to 2 g of powdered tissue. The lysate was clarified and incubated with GFP-Trap (Chromtek) for 3 h at 4°C. Beads were magnetically separated from the lysate and washed 5 times in wash buffer (50 mM Tris-Cl, pH 7.4; 150 mM KCl, 1 mM phenylmethylsulfonyl fluoride). The buffer was completely removed and 3× sodium dodecyl sulfate sample dye was added to the beads and incubated at 70°C for 10 min. The pull-down products were resolved in 4–20% Tris-glycine sodium dodecyl sulfate gradient gels (Bio-Rad).

Mass spectrometry

In-solution digestion of the purified protein was performed using 13 ng μl^{-1} trypsin in 10 mM ammonium bicarbonate containing 10% (v/v) acetonitrile. Approximately 50 ng of the prepared samples was subjected to liquid chromatography/tandem MS, using a LTQ Orbitrap XL (Thermo Scientific), higher-energy C-trap dissociation activation, C-18 column, 15 cm length. The data were analyzed using Proteome Discoverer (Thermo Scientific). For peptide identification, Sequest HT search engine was used against the combined target-decoy database with the following parameters: enzyme: trypsin; maximum missed cleavage: 2; variable modifications: oxidation. Search tolerance parameters were as follows: minimum peptide length; 6, maximum; 144, false discovery rate, <1%.

Viral replication assay and Southern blotting

Viral titer assay was performed as previously shown (Nair et al., 2020; Shivaprasad et al., 2006; Shivaprasad et al., 2008). Partial dimer of SyYVCV DNA-A, DNA-β, and 35S driven plasmids were mobilized into *Agrobacterium* strain LBA4404 (pSB1) and co-infiltrated alone or in various combinations into *N. tabacum* leaves. Genomic DNA from infiltrated and systemic leaves were isolated using the CTAB method (Rogers and Bendich, 1994). An equal amount of genomic DNA normalized using Qubit and gel-based quantification was loaded onto a 0.7% TNE agarose gel and resolved at 5 V cm^{-1}. The transfer was performed as previously mentioned (Shivaprasad et al., 2006) and blots were probed with full-length DNA-A in case of replication assay and *psbM* gene probe (3 kb) for plastid Southern blot. The probes were internally labeled with dCTP alpha P32 (BRIT, India) using the Rediprime II kit (GE). Blots were scanned using Typhoon Trio Scanner (GE) in phosphorescence mode.

Y2H transformation and screening

Yeast transformation was performed as described with minor modifications (Gietz & Woods, 2002). Freshly streaked AH109 cells were used to initiate primary culture grown overnight in YPD media (yeast extract 1%, bacterial peptone 2%, and dextrose 2%). Cells were grown to A600 = 0.6 OD. About 10 ml of cells were pelleted per transformation. The freshly pelleted cells were transferred to a 1.5 ml centrifuge tube and washed with deionized sterile water followed by 0.1 M lithium acetate. Transformation mixture (PEG 3000 50%, salmon sperm DNA, and lithium acetate) was added to the washed cells, and cells were resuspended. The corresponding mixture of AD and BD plasmids was added to the transformation mixture followed by vortexing for 30 sec. The mixture was incubated for 30 min at 30°C and 30 min at 42°C. The reaction mixture was removed and cells were resuspended in 2 ml YPD media and allowed to recover for 2 h before plating onto an auxotrophic media. Transformants were screened on -Leu, -Trp media followed by screening for interaction on -Leu, -Trp, -His with or without 3-AT (Sigma-Aldrich).

Electrophoretic mobility shift assay

Electrophoretic mobility shift assay (EMSA) was performed as previously described (Csorba & Burgyán, 2011). Briefly, oligos were end-labeled using T4 polynucleotide kinase (NEB) with γ-32P. Labeled oligos were diluted as mentioned for each experiment typically to 100–200 pg. Labeled oligos were incubated with protein in EMSA binding buffer (50 mM Tris-Cl pH 8, 100 mM NaCl, 5% glycerol) for a specific time interval as detailed in the experiment followed by stopping the reaction by addition of non-denaturing stop-dye. The reaction was further resolved in an 8% native TBE gel and exposed to a phosphor screen for development. The phosphor screen was scanned using Typhoon trio plus (GE) and the image was analyzed using FIJI. For nuclease assay, buffer contained 50 mM Tris-Cl pH 8, 100 mM NaCl, 5% glycerol, and 5 mM Mg^{2+}.

ACCESSION NUMBERS

RNA-Seq data are available under GEO accession number: GSE189526.

AUTHOR CONTRIBUTIONS

AN and PVS designed the study, analyzed the data and wrote the manuscript. AN performed almost all the experiments. CYH helped with PVX and tobacco transgenics. ANN helped with transcriptome analysis.

ACKNOWLEDGMENTS

We thank members of Shivaprasad lab for suggestions. We thank the Next Generation Genomics, radiation, greenhouse, CIFF and mass-spec at NCBS-TIFR, Bangalore. We thank Dr. Anjana Badrinarayanan and Afroze C. for critical discussion on RecA function and for cvRecA antibody. We also thank Prof. K. Veluthambi for binary vectors and *Agrobacterium* strains. We thank Prof. Supriya Chakraborty for PVX construct. This study was supported by Department of Atomic Energy, Government of India, under Project Identification No. RTI 4006 (1303/3/2019/R&D-II/DAE/4749 dated 16.7.2020). ANN acknowledges a fellowship from DBT, India. This work was also supported by NCBS-TIFR core funding and grants (BT/PR12394/AGIII/103/891/2014;BT/IN/Swiss/47/JGK/2018-19; BT/PR25767/GET/119/151/2017) from Department of Biotechnology, Government of India.

CONFLICT OF INTEREST

The authors declare no conflicts of interest.

DATA AVAILAIBLITY STATEMENT

All data generated or analyzed during this study are included in this published article (and its supplementary information files). RNA-Seq data are available under GEO accession number: GSE189526.

SUPPORTING INFORMATION

Additional Supporting Information may be found in the online version of this article.

Figure S1. Signaling pathways are deregulated in βC1 transgenic lines.

Figure S2. Plastid localized genes are significantly misexpressed in βC1-OE lines.

Figure S3. βC1 binds preferably to ssDNA *in vitro*.

Figure S4. Size exclusion profile of βC1 and its truncation mutants.

Figure S5. Plant RecA, a Rad51 homolog, is essential for cell survival in presence of βC1.

Figure S6. RecA directly interacts with SyYVCV βC1.

Figure S7. NtRecA1 binds to DNA.

Figure S8. RecA1 enhances viral replication in the presence of βC1.

Table S1. Mass spectrometry identified interacting proteins in *E. coli* purified βC1.

Table S2. List of primers used in this study.

Table S3. List of clones used in this study.

Table S4. List of sequence IDs used to construct clones.

Table S5. List of antibodies and IP materials used in this study.

REFERENCES

Ascencio-Ibáñez, J.T., Sozzani, R., Lee, T.-J., Chu, T.-M., Wolfinger, R.D., Cella, R. *et al.* (2008) Global analysis of Arabidopsis gene expression uncovers a complex Array of changes impacting pathogen response and cell cycle during Geminivirus infection. *Plant Physiology*, **148**, 436–454.

Bendich, A.J. (1987) Why do chloroplasts and mitochondria contain so many copies of their genome? *BioEssays*, **6**, 279–282.

Bhattacharyya, D., Gnanasekaran, P., Kumar, R.K., Kushwaha, N.K., Sharma, V.K., Yusuf, M.A. *et al.* (2015) A geminivirus betasatellite damages the structural and functional integrity of chloroplasts leading to symptom formation and inhibition of photosynthesis. *Journal of Experimental Botany*, **66**, 5881–5895.

Briddon, R.W., Bull, S.E., Amin, I., Idris, A.M., Mansoor, S., Bedford, I.D. *et al.* (2003) Diversity of DNA β, a satellite molecule associated with some monopartite begomoviruses. *Virology*, **312**, 106–121.

Cerutti, H., Osman, M., Grandoni, P. & Jagendorf, A.T. (1992) A homolog of Escherichia coli RecA protein in plastids of higher plants. *Proceedings of the National Academy of Sciences of the United States of America*, **89**, 8068–8072.

Chan, K.X., Crisp, P.A., Estavillo, G.M. & Pogson, B.J. (2010) Chloroplast-to-nucleus communication. *Plant Signaling & Behavior*, **5**, 1575–1582.

Chandran, D., Rickert, J., Huang, Y., Steinwand, M.A., Marr, S.K. & Wildermuth, M.C. (2014) Atypical E2F transcriptional repressor DEL1 acts at the intersection of plant growth and immunity by controlling the hormone salicylic acid. *Cell Host & Microbe*, **15**, 506–513.

Cheng, X., Wang, X., Wu, J., Briddon, R.W. & Zhou, X. (2011) βC1 encoded by tomato yellow leaf curl China betasatellite forms multimeric complexes in vitro and in vivo. *Virology*, **409**, 156–162.

Csorba, T. & Burgyán, J. (2011) Gel mobility shift assays for RNA binding viral RNAi suppressors. *Methods in Molecular Biology*, **721**, 245–252.

Cui, X., Tao, X., Xie, Y., Fauquet, C.M. & Zhou, X. (2004) A DNAβ associated with tomato yellow leaf curl China virus is required for symptom induction. *Journal of Virology*, **78**, 13966–13974.

Das, S., Hegde, A. & Shivaprasad, P.V. (2018) Molecular characterization of a new begomovirus infecting Synedrella nodiflora in South India. *Archives of Virology*, **163**, 2551–2554.

Day, A. & Madesis, P. (2007) DNA replication, recombination, and repair in plastids. *Topics in Current Genetics*, **19**, 65–119.

de Torres Zabala, M., Littlejohn, G., Jayaraman, S., Studholme, D., Bailey, T., Lawson, T. *et al.* (2015) Chloroplasts play a central role in plant defence and are targeted by pathogen effectors. *Nature Plants*, **1**(15), 74.

Eberhard, S., Drapier, D. & Wollman, F.-A. (2002) Searching limiting steps in the expression of chloroplast-encoded proteins: relations between gene copy number, transcription, transcript abundance and translation rate in the chloroplast of Chlamydomonas reinhardtii. *The Plant Journal*, **31**, 149–160.

Fondong, V.N., Reddy, R.V.C., Lu, C., Hankoua, B., Felton, C., Czymmek, K. *et al.* (2007) The consensus N -Myristoylation motif of a Geminivirus AC4 protein is required for membrane binding and pathogenicity. *Molecular Plant-Microbe Interactions*, **20**, 380–391.

Gietz, R.D. & Woods, R.A. (2002) Transformation of yeast by lithium acetate/single-stranded carrier DNA/polyethylene glycol method. *Methods in Enzymology*, **350**, 87–96.

Gnanasekaran, P., Ponnusamy, K. & Chakraborty, S. (2019) A geminivirus betasatellite encoded βC1 protein interacts with PsbP and subverts PsbP-mediated antiviral defence in plants. *Molecular Plant Pathology*, **20**, 943–960.

Golczyk, H., Greiner, S., Wanner, G., Weihe, A., Bock, R., Börner, T. *et al.* (2014) Chloroplast DNA in mature and senescing leaves: A reappraisal. *The Plant Cell*, **26**, 847–854.

Hanley-Bowdoin, L., Bejarano, E.R., Robertson, D. & Mansoor, S. (2013) Geminiviruses: masters at redirecting and reprogramming plant processes. *Nature Reviews Microbiology*, **11**, 777–788.

Heyraud, F., Matzeit, V., Kammann, M., Schaefer, S., Schell, J. & Gronenborn, B. (1993) Identification of the initiation sequence for viral-strand DNA synthesis of wheat dwarf virus. *The EMBO Journal*, **12**, 4445–4452.

Heyraud-Nitschke, F., Schumacher, S., Laufs, J., Schaefer, S., Schell, J. & Gronenborn, B. (1995) Determination of the origin cleavage and joining domain of geminivirus rep proteins. *Nucleic Acids Research*, **23**, 910–916.

Hosler, J.P., Wurtz, E.A., Harris, E.H., Gillham, N.W. & Boynton, J.E. (1989) Relationship between gene dosage and gene expression in the chloroplast of *Chlamydomonas reinhardtii*. *Plant Physiology*, **91**, 648–655.

Inouye, T., Odahara, M., Fujita, T., Hasebe, M. & Sekine, Y. (2008) Expression and complementation analyses of a chloroplast-localized homolog of bacterial RecA in the Moss *Physcomitrella patens*. *Bioscience, Biotechnology, and Biochemistry*, **72**, 1340–1347.

Jeske, H., Lütgemeier, M. & Preiß, W. (2001) DNA forms indicate rolling circle and recombination-dependent replication of abutilon mosaic virus. *EMBO Journal*, **20**, 6158–6167.

Jha, V., Narjala, A., Basu, D., Sujith, T.N., Pachamuthu, K., Chenna, S. *et al.* (2021) Essential role of γ-clade RNA-dependent RNA polymerases in rice development and yield-related traits is linked to their atypical polymerase activities regulating specific genomic regions. *New Phytologist*, **232**, 1674–1691.

Kaliappan, K., Choudhury, N.R., Suyal, G. & Mukherjee, S.K. (2012) A novel role for RAD54: this host protein modulates geminiviral DNA replication. *The FASEB Journal*, **26**, 1142–1160.

Khazi, F.R., Edmondson, A.C. & Nielsen, B.L. (2003) An Arabidopsis homologue of bacterial RecA that complements an E. coli recA deletion is targeted to plant mitochondria. *Molecular Genetics and Genomics*, **269**, 454–463.

Kim, D., Paggi, J.M., Park, C., Bennett, C. & Salzberg, S.L. (2019) Graph-based genome alignment and genotyping with HISAT2 and HISAT-genotype. *Nature Biotechnology*, **37**, 907–915.

Kunkel, T.A. (2004) DNA replication fidelity. *Journal of Biological Chemistry*, **279**, 16895–16898.

León, J. & Sánchez-Serrano, J.J. (1999) Molecular biology of jasmonic acid biosynthesis in plants. *Plant Physiology and Biochemistry*, **37**, 373–380.

Majeran, W., Friso, G., Asakura, Y., Qu, X., Huang, M., Ponnala, L. *et al.* (2012) Nucleoid-enriched proteomes in developing plastids and chloroplasts from maize leaves: A new conceptual framework for nucleoid functions. *Plant Physiology*, **158**, 156–189.

Martin, M. (2011) Cutadapt removes adapter sequences from high-throughput sequencing reads. *EMBnet.Journal*, **17**, 10.

Maslowska, K.H., Makiela-Dzbenska, K. & Fijalkowska, I.J. (2019) The SOS system: A complex and tightly regulated response to DNA damage. *Environmental and Molecular Mutagenesis*, **60**, 368–384.

Medina-Puche, L., Tan, H., Dogra, V., Wu, M., Rosas-Diaz, T., Wang, L. *et al.* (2020) A defense pathway linking plasma membrane and chloroplasts and Co-opted by pathogens. *Cell*, **182**, 1109–1124.e25.

Mi, H., Ebert, D., Muruganujan, A., Mills, C., Albou, L.-P., Mushayamaha, T. *et al.* (2021) PANTHER version 16: a revised family classification, tree-based classification tool, enhancer regions and extensive API. *Nucleic Acids Research*, **49**, D394–D403.

Nair, A., Chatterjee, K.S., Jha, V., Das, R. & Shivaprasad, P.V. (2020) Stability of begomoviral pathogenicity determinant βC1 is modulated by mutually antagonistic SUMOylation and SIM interactions. *BMC Biology*, **18**, 110.

Nambara, E. & Marion-Poll, A. (2005) Abscisic acid biosynthesis and catabolism. *Annual Review of Plant Biology*, **56**, 165–185.

Nomura, H., Komori, T., Uemura, S., Kanda, Y., Shimotani, K., Nakai, K. *et al.* (2012) Chloroplast-mediated activation of plant immune signalling in Arabidopsis. *Nature Communications*, **3**, 926.

Odahara, M., Inouye, T., Nishimura, Y. & Sekine, Y. (2015) RECA plays a dual role in the maintenance of chloroplast genome stability in *Physcomitrella patens*. *The Plant Journal*, **84**, 516–526.

Odahara, M., Kishita, Y. & Sekine, Y. (2017) MSH1 maintains organelle genome stability and genetically interacts with *RECA* and *RECG* in the moss *Physcomitrella patens*. *The Plant Journal*, **91**, 455–465.

Odahara, M., Masuda, Y., Sato, M., Wakazaki, M., Harada, C., Toyooka, K. *et al.* (2015) RECG maintains plastid and mitochondrial genome stability by suppressing extensive recombination between short dispersed repeats. *PLOS Genetics*, **11**, e1005080.

Padmanabhan, M.S. & Dinesh-Kumar, S.P. (2010) All hands on deck—the role of chloroplasts, endoplasmic reticulum, and the nucleus in driving plant innate immunity. *Molecular Plant-Microbe Interactions*, **23**, 1368–1380.

Pérez-Amador, M.A., Abler, M.L., De Rocher, E.J., Thompson, D.M., van Hoof, A., LeBrasseur, N.D. *et al.* (2000) Identification of BFN1, a bifunctional nuclease induced during leaf and stem senescence in Arabidopsis. *Plant Physiology*, **122**, 169–180.

Preiss, W. & Jeske, H. (2003) Multitasking in replication is common among Geminiviruses. *Journal of Virology*, **77**, 2972–2980.

Rauwolf, U., Golczyk, H., Greiner, S. & Herrmann, R.G. (2010) Variable amounts of DNA related to the size of chloroplasts III. Biochemical determinations of DNA amounts per organelle. *Molecular Genetics and Genomics*, **283**, 35–47.

Richter, K.S., Serra, H., White, C.I. & Jeske, H. (2016) The recombination mediator RAD51D promotes geminiviral infection. *Virology*, **493**, 113–127.

Rizvi, I., Choudhury, N.R. & Tuteja, N. (2015) Insights into the functional characteristics of geminivirus rolling-circle replication initiator protein and its interaction with host factors affecting viral DNA replication. *Archives of Virology*, **160**, 375–387.

Rowan, B.A., Oldenburg, D.J. & Bendich, A.J. (2010) RecA maintains the integrity of chloroplast DNA molecules in Arabidopsis. *Journal of Experimental Botany*, **61**, 2575–2588.

Sakamoto, W. & Takami, T. (2018) Chloroplast DNA dynamics: copy number, quality control and degradation. *Plant and Cell Physiology*, **59**, 1120–1127.

Sato, N., Terasawa, K., Miyajima, K. & Kabeya, Y. (2003) Organization, developmental dynamics, and evolution of plastid nucleoids. *International Review of Cytology*, **232**, 217–262.

Schmid, M., Speiseder, T., Dobner, T. & Gonzalez, R.A. (2014) DNA virus replication compartments. *Journal of Virology*, **88**, 1404–1420.

Serrano, I., Audran, C. & Rivas, S. (2016) Chloroplasts at work during plant innate immunity. *Journal of Experimental Botany*, **67**, 3845–3854.

Shivaprasad, P.V., Rajeswaran, R., Blevins, T., Schoelz, J., Meins, F., Hohn, T. *et al.* (2008) The CaMV transactivator/viroplasmin interferes with RDR6-dependent trans-acting and secondary siRNA pathways in Arabidopsis. *Nucleic Acids Research*, **36**, 5896–5909.

Shivaprasad, P.V., Thillaichidambaram, P., Balaji, V. & Veluthambi, K. (2006) Expression of full-length and truncated rep genes from Mungbean yellow mosaic virus-Vigna inhibits viral replication in transgenic tobacco. *Virus Genes*, **33**, 365–374.

Stanley, J. (1995) Analysis of African cassava mosaic virus recombinants suggests strand nicking occurs withinthe conserved nonanucleotide motif during the initiation of rolling circle DNA replication. *Virology*, **206**, 707–712.

Sung, Y.K. & Coutts, R.H.A. (1996) Potato yellow mosaic geminivirus AC2 protein is a sequence non-specific DNA binding protein. *FEBS Letters*, **383**, 51–54.

Sunilkumar, G., Vijayachandra, K. & Veluthambi, K. (1999) Preincubation of cut tobacco leaf explants promotes agrobacterium-mediated transformation by increasing vir gene induction. *Plant Science*, **141**, 51–58.

Takami, T., Ohnishi, N., Kurita, Y., Iwamura, S., Ohnishi, M., Kusaba, M. *et al.* (2018) Organelle DNA degradation contributes to the efficient use of phosphate in seed plants. *Nature Plants*, **4**, 1044–1055.

Tang, L.Y. & Sakamoto, W. (2011) Tissue-specific organelle DNA degradation mediated by DPD1 exonuclease. *Plant Signaling & Behavior*, **6**, 1391–1393.

Trapnell, C., Williams, B., Pertea, G., Mortazavi, A., Kwan, G., Baren, M.J. *et al.* (2011) Transcript assembly and abundance estimation from RNA-seq reveals thousands of new transcripts and switching among isoforms. *Nature Biotechnology*, **28**, 511–515.

Udy, D.B., Belcher, S., Williams-Carrier, R., Gualberto, J.M. & Barkan, A. (2012) Effects of reduced chloroplast gene copy number on chloroplast gene expression in maize. *Plant Physiology*, **160**, 1420–1431.

Wang, W., Vignani, R., Scali, M. & Cresti, M. (2006) A universal and rapid protocol for protein extraction from recalcitrant plant tissues for proteomic analysis. *Electrophoresis*, **27**, 2782–2786.

Wang, Y., Gong, Q., Wu, Y., Huang, F., Ismayil, A., Zhang, D. *et al.* (2021) A calmodulin-binding transcription factor links calcium signaling to antiviral RNAi defense in plants. *Cell Host & Microbe*, **29**, 1393–1406.e7.

Wildermuth, M.C., Dewdney, J., Wu, G. & Ausubel, F.M. (2001) Isochorismate synthase is required to synthesize salicylic acid for plant defence. *Nature*, **414**, 562–565.

Yang, J.-Y., Iwasaki, M., Machida, C., Machida, Y., Zhou, X. & Chua, N.-H. (2008) βC1, the pathogenicity factor of TYLCCNV, interacts with AS1 to alter leaf development and suppress selective jasmonic acid responses. *Genes & Development*, **22**, 2564–2577.